European Journal of Neurology

WILEY | ean

ORIGINAL ARTICLE OPEN ACCESS

Genetic ALS—Progressive Sleep Defects Precede the Onset of Clinical Disease

Christina Lang[1,2] | Simon J. Guillot[3] | Antje Knehr[1] | Patrick Weydt[4] | Johannes Dorst[1] | Hayrettin Tumani[1] | Albert C. Ludolph[1,5] | Luc Dupuis[3] | Matei Bolborea[3]

[1]Department of Neurology, University Hospital of Ulm, Ulm, Germany | [2]Deutsches Zentrum für Neurodegenerative Erkrankungen (DZNE), Ulm, Germany | [3]University of Strasbourg, INSERM, Strasbourg Translational Neuroscience & Psychiatry STEP - CRBS, UMR-S 1329, Strasbourg, France | [4]Deutsches Zentrum für Neurodegenerative Erkrankungen (DZNE), Bonn, Germany | [5]Institute of Applied Physiology, University of Ulm, Ulm, Germany

Correspondence: Albert C. Ludolph (albert.ludolph@uni-ulm.de) | Luc Dupuis (ldupuis@unistra.fr) | Matei Bolborea (mbolborea@unistra.fr)

Received: 31 March 2026 | **Revised:** 13 July 2026 | **Accepted:** 4 September 2026

Keywords: *C9orf72* | electroencephalography | polysomnography | *SOD1*

ABSTRACT

Background: The onset of amyotrophic lateral sclerosis (ALS) is preceded by non-motor signs detectable many years before motor symptom onset. We recently showed that early ALS patients and presymptomatic carriers of ALS-associated gene mutations display altered sleep macroarchitecture, characterised by increased wakefulness and decreased non-REM sleep, together with altered microarchitecture, particularly reduced slow oscillations and sleep spindles. Here we aimed at determining whether sleep alterations are progressive in premanifest carriers of ALS-associated gene mutations.

Methods: This longitudinal observational cohort study included presymptomatic first-degree relatives of ALS patients carrying pathogenic gene mutations ($n = 18$) and noncarrier family members ($n = 3$). Sleep macroarchitecture and sleep microarchitecture were assessed using standardised polysomnography and electroencephalographic analyses at baseline and in a follow-up examination after 2.3 ± 1.5 years.

Results: In all carriers, sleep alterations were more severe at follow-up compared to the initial examination, for both macro- and microarchitecture. The progression of sleep alterations was seemingly independent of proximity to motor onset, whether evaluated by increased neurofilament levels or phenoconversion during the study period.

Conclusions: Sleep macro- and microarchitectural abnormalities progressively worsen during the premanifest phase of ALS. These findings suggest that polysomnography-derived sleep measures and their neurochemical correlates may serve as sensitive, noninvasive surrogate biomarkers of disease progression in clinically silent ALS. This could support disease prevention, for example, by the antisense oligonucleotide tofersen in patients carrying SOD1 mutations.

1 | Introduction

Amyotrophic lateral sclerosis (ALS) is the most common adult-onset motor neuron disease, resulting from combined degeneration of upper and lower motor neurons and leading to progressive paralysis and premature death, typically three to four years after the onset of motor symptoms. Onset usually occurs between 60 and 70 years of age [1, 2] and most cases are sporadic, without a known family history. Between 5 and 10% of ALS cases are caused by mutations in more than 40 distinct genes, usually

Christina Lang and Simon J. Guillot contributed equally to this article.

This is an open access article under the terms of the Creative Commons Attribution-NonCommercial-NoDerivs License, which permits use and distribution in any medium, provided the original work is properly cited, the use is non-commercial and no modifications or adaptations are made.

© 2026 The Author(s). *European Journal of Neurology* published by John Wiley & Sons Ltd on behalf of European Academy of Neurology.

through autosomal dominant inheritance. In Europe, the most frequent mutations are found in *C9orf72, SOD1*, *TARDBP*, and *FUS* genes [1, 2].

In ALS gene carriers, definite motor symptom onset is usually preceded by a prodromal period that may include mild motor impairment. During this prodromal period, an increase in circulating neurofilament levels, a reliable biomarker of axonal injury, has been reported [3, 4]. Before this highly variable prodromal period, presymptomatic gene carriers do not show any motor impairment either clinically or through biomarker evidence [4]. However, many studies indicate that these individuals already exhibit non-motor signs, such as weight loss [5] or cognitive impairment [6], many years before motor symptom onset, during the premanifest period of the disease. Whether these early non-motor signs worsen as individuals approach disease onset remains unclear, largely due to the lack of longitudinal studies in presymptomatic gene carriers.

We recently demonstrated that sleep is impaired in ALS, both in the clinically manifest period and in premanifest gene carriers. Specifically, prominent defects in sleep macroarchitecture were observed and characterised by increased wake and decreased deep sleep (NREM2/3) [7]. These defects were present in symptomatic patients in the absence of detectable respiratory insufficiency. They were accompanied by marked defects in microarchitecture, particularly decreased slow oscillations and sleep spindles [8]. Importantly, similar impairments were observed in presymptomatic gene carriers many years before manifest disease. These sleep alterations correlated with cognitive scores [7], and both macro- and microarchitectural changes were also observed in multiple mouse models of familial ALS [7, 8].

A major question arising from these initial studies is whether sleep defects—macro- or microarchitecture—remain stable as individuals approach disease onset, or whether they worsen, suggesting an association with rampant disease progression. This could make a prediction of disease onset possible. In this study, we performed longitudinal follow-up polysomnography in 18 presymptomatic ALS gene carriers and in three family members with negative genetic testing previously included in our initial studies.

2 | Methods and Materials

2.1 | Design

Longitudinal prospective observational study.

2.2 | Setting and Participants

All participants in this study are first-degree relatives of fALS patients with an ALS-causing mutation confirmed by genetic testing who were seen at the outpatient clinic for motor neuron diseases or in the neurology department of Ulm University Hospital between 2019 and 2024. This cohort has been previously described [7, 8]. Relatives of these patients were informed of the opportunity to participate in the study. Inclusion criteria were: Age 18 years or older and being a first-degree relative of a confirmed fALS case. The exclusion criterion was the presence of a neurodegenerative disease or other serious illness, as well as a relationship to another study participant; further, an Apnea-Hypopnoe-Index (AHI) greater than 20 per hour or a Periodic-Limb-Movement-Index greater than 20 per hour in the baseline polysomnography led to the exclusion of the participant. Study participants did not undergo genetic testing at the time of inclusion in the study. Genetic testing was performed purely for scientific purposes and for later classification. Participants who wished to undergo official predictive genetic testing had to do so outside the study, after the first study visit, in accordance with the provisions of the German Genetic Diagnosis Act.

Medical history and current medication use were documented as part of the clinical assessment. Individuals with relevant medical or psychiatric conditions or medication use that, in the opinion of the investigators, could substantially interfere with sleep assessment or study participation were not included. Phenoconversion was defined as the occurrence of clinically evident ALS-related signs or symptoms in a previously presymptomatic gene carrier, supported by electromyographic findings. Biomarker abnormalities, including NfL levels, were not used to define phenoconversion.

2.3 | Ethical standards

The study was conducted in accordance with the Declaration of Helsinki (revised version) and approved by the Ethics Committee of Ulm University (approval number: 68/19).

2.4 | Electroencephalography in Subjects

All participants underwent two visits, each including a one-night full polysomnography according to the American Academy of Sleep Medicine (AASM) guidelines [9], with monitoring of various physiological parameters, including electroencephalogram (EEG), surface electromyogram (EMG), electrooculogram (EOG), electrocardiogram (ECG), respiratory effort and flow, pulse, and oxygen saturation. EEG electrodes were placed according to the international 10–20 system. The following electrodes were used in each subject: Fz, C3, C4, Cz, P3, P4, Pz, O1, O2, A1, and A2. The sampling rate was 512 Hz in each case. A "*lights off*" marker was placed in each recording to indicate when the participant turned off the lights and attempted to sleep. Participants were free to choose a start time between 8:00 p.m. and midnight. The measurement ended at 6:00 a.m. Two volunteers underwent an additional third polysomnography under the same protocol.

2.5 | EEG Preprocessing

Analyses were performed using available Python packages (Python Software Foundation. Python Language Reference, version 3.12. Available at http://www.python.org) relying on the MNE package. EEG preprocessing followed established protocols [7, 8]. Recordings were first de-identified using the open-source Prerau Lab EDF De-identification Tool (Version 1.0; 2023) in Python (Prerau Lab EDF De-identification Tool retrieved from https://sleepeeg.org/edf-de-identification-tool),

concealing mutation and visit number prior to further analysis. Signals were then notch-filtered to remove the 50 Hz power line. Independent component analysis was applied to remove residual artefacts, which were then excluded upon visual inspection while being blinded to genotype and visit number, based on standard criteria (ocular topography, muscle-related high-frequency power), as described [7, 8].

2.6 | Analysis of Sleep Macroarchitecture

Analyses focused on the sensorimotor cortices (C_3 and C_4), which are known to be impaired at disease onset, as well as nearby interhemispheric sulci (Fz, Cz and Pz). Sleep staging was performed on a 6-h window with 30-s epochs, starting at lights off, using the YASA deep learning algorithm (v0.6.5) [10] and spectral analysis. Time in bed and total sleep time were calculated across the full recording. Automated sleep staging, hypnograms, and spectrograms were generated using Welch's method as described [7, 8]. Sleep pressure was quantified using the area under the curve (AUC) of delta power (0.5–4 Hz) of the first hour of the 6-h window, computed using Simpson's rule. REM efficiency was calculated as the ratio of theta power (4–8 Hz) to delta power (0.5–4 Hz) during REM epochs. Sleep staging and analysis followed AASM guidelines [9].

2.7 | Analyses of Sleep Microarchitectural Events

Analyses were performed as in our previous study [8]. Briefly, sleep spindles, slow oscillations, and K-complexes were analysed across all electrodes, with outliers removed using an isolation forest algorithm [8]. K-complex analysis was restricted to the sensorimotor cortex (C3), which is known to be impaired in ALS, using the MNE and SciPy packages [8]. Sleep spindle density was defined as the number of sleep spindles per minute of NREM2 sleep. Slow oscillation density was defined as the number of slow oscillations per minute of NREM2 sleep. K-complex density was defined as the number of K-complexes per minute of NREM2 sleep. All analyses were performed in accordance with AASM guidelines [9].

2.8 | Measurement of Neurofilament Light Chain Levels

Blood samples were collected by venous sampling. Samples were centrifuged at 2000 g for 10 min, and the extracted serum was aliquoted and frozen within 30 min at −80°C. Serum samples were stored in polypropylene tubes. For NF-L quantification in serum, the microfluidic Ella platform (Bio-Techne, Minneapolis, USA) was used. The analyses were performed according to the manufacturer's instructions [11].

2.9 | Statistical Analysis

Prior to any statistical analysis, normality and homoscedasticity were tested using the Shapiro–Wilk test and Bartlett's test, respectively. Follow-up analyses were performed using paired *t*-tests or Wilcoxon-Mann–Whitney rank-sum tests when normality was not met.

For longitudinal analyses, each sleep variable was modelled using a linear mixed-effects framework, with visit (visit 1 vs. visit 2) and interval between visits as fixed effects, and case treated as a random factor to account for repeated measures. Analyses were performed separately for the *C9orf72* group, *SOD1* group, other mutations, and the full cohort.

In all cases, p_{value} were adjusted using FDR-BKY correction. Data are presented as violin plots with each value displayed as a data point and expressed as medians ± interquartile range. Visualisations were generated using Seaborn and Matplotlib packages. Results were deemed significant at adjusted $p_{value} < 0.05$, and only corrected p_{values} (adj. p_{value}) are reported.

3 | Results

In the original baseline study, 61 participants were examined, including 35 gene carriers and 26 non-carriers from the family. From this cohort, 15 participants were excluded from the present longitudinal analysis based on the predefined exclusion criteria. Of the remaining eligible participants, 18 gene carriers and 3 non-carrier controls could be re-invited and underwent follow-up assessment.

The study population is described in Table 1 and includes 18 presymptomatic gene carriers, with *C9orf72* ($n = 12$), *SOD1* ($n = 3$), *FUS* ($n = 2$), and *TARDBP* ($n = 1$). We also included $n = 3$ non-carrier individuals who were negative for gene testing. All volunteers had an initial polysomnography in a previous study [7, 8]. The second visit occurred 2.3 ± 1.5 years after the first visit (range: 0.3–5.2 years). Two individuals underwent a third polysomnography, including one who phenoconverted to clinically manifest ALS. Age at disease onset of the affected first-degree relative was not documented in seven participants because contact with the affected relative with ALS had been lost or because the timing of first symptoms could not be reliably determined retrospectively.

Follow-up intervals between Visit 1 and subsequent assessments varied between participants. This variability was mainly due to the limited flexibility for scheduling repeated hospital-based polysomnographic recordings in clinically healthy gene carriers. Individual follow-up intervals are shown in Table 1.

3.1 | Progressive Changes in Sleep Macroarchitecture

Polysomnography results were analysed using the YASA deep learning algorithm [10], over a 6-h window following lights off. Hypnograms of two representative premanifest gene carriers (one *C9orf72* and one *SOD1*) at visit 1 and visit 2 are shown in Figure 1, with quantitative results in Figure 2 and Table 2. There was a systematic increase in the percentage of wake (Figure 2A) across all 18 subjects, while rapid eye movement (REM) sleep (Figure 2B) and non-rapid eye movement (NREM) sleep (Figure 2C) showed heterogeneous variations across volunteers. Interestingly, when NREM stage was subdivided into NREM1, 2, and 3, we observed a clear

TABLE 1 | Descriptive table of the study population of presymptomatic gene carriers.

Case	Classification	Age at visit 1	Gender	Gene	Mutation details	Age at onset of index case	NFL i.S. visit 1 (pg/mL) (z-score)	NFL i.S. visit 2 (pg/mL) (z-Score)	Time between visit 1 & 2 (years)	Time between visit 2 & 3 (years)	Phenoconversion	AHI visit 1 (/h)	PLMSI visit 1(/h)
01	Carrier	27	W	*TARDBP*	p.N378A382del	33	—	—	5.1	—		0.3	0.6
02	Carrier	51	W	*C9ORF72*	1100–1950	53	—	—	5.2	—		4.6	0.0
03	Carrier	25	M	*C9ORF72*	1700–2400	50	6 (0.07)	6 (−0.16)	4.3	—		2.7	7.0
04	Carrier	22	M	*C9ORF72*	1550–2100	50	10 (1.06)	10 (0.9)	4.8	—		1.6	0.7
05	Carrier	17	W	*FUS*	p.G504Wfs*12	—	17 (1.88)	7 (0.49)	4.8			1.7	13.5
06	Carrier	47	M	*SOD1*	E100K	50	40 (2.18)	46 (2.27)	3.1	—		5.3	14.8
07	Carrier	29	W	*FUS*	p.R514T	49	10 (0.85) CSF: 303 (0.25)	8 (0.13) CSF: 764 (1.7)	2.1	1.2	Yes	2.1	0.0
08	Control	47	W	*C9ORF72*	—	65	16 (−0.2)	8 (−1.77)	2.1	—		15.3	19.8
09	Carrier	33	W	*C9ORF72*	> 60	—	11 (0.89)	13 (1.06)	1.2	0.7		9.3	1.4
10	Carrier	38	W	*C9ORF72*	1300–1700	60	—	—	2.1	—		1.6	21.5
11	Carrier	47	M	*C9ORF72*	650–800	53	33(1.88)	10 (−0.77)	1.8	—		3.6	2.8
12	Control	38	M	*GRN*		63	11 (0.08)	5 (−1.43)	1.9	—		2.7	1.3
14	Carrier	60	W	*C9ORF72*	1350–1800	—	7 (−1.99)	14 (−1.15)	2.2	—		11.9	27.5
15	Control	48	W	*C9ORF72*	—	70	20 (0.84)	16 (0.25)	1.5	—		2.5	4.3
16	Carrier	35	W	*SOD1*	p.R116G	43	16 (1.26)	9 (0.04)	1.4	—		2.5	3.7
17	Carrier	32	W	*SOD1*	p.R116G	43	—	6 (−0.29)	1.4	—		1.4	1.4
18	Carrier	31	W	*C9ORF72*	1300–1700	—	—	—	0.3	—		1.6	0.6
19	Carrier	44	W	*C9ORF72*	1600–2000	60	16 (0.65)	15 (0.44)	0.9	—		2.2	3.8
20	Carrier	29	W	*C9ORF72*	> 60	—	8 (0.43)	8 (0.39)	1.0	—		0.3	1.8
21	Carrier	31	M	*C9ORF72*	> 60	—	14 (1.28)	12 (1.05)	1.0	—		3.9	1.8
22	Carrier	41	W	*C9ORF72*	1100–1600	—	16 (0.0.89)	11 (0.01)	1.0	—		7.6	10.6

Note: For C9orf72 gene carriers, the mutation details indicate the approximate number of hexanucleotide repeats. For three participants, the number of repeats was not classified, but only examined to determine whether there was a repeat expansion; in these cases, this is indicated with "> 60".
Abbreviations: W: woman; M: man.

increase in NREM1 (light sleep) at the expense of NREM3 (deep sleep) (Figure 2D–F). Consistent with a worsening of the initial sleep phenotype, an augmentation in sleep onset latency (Figure 2G), a reduction in sleep efficiency (Figure 2H), a decline in sleep maintenance efficiency (Figure 2I), a decrease in REM efficiency (Figure 2J), an increase in sleep pressure (Figure 2K), and an increase in sleep fragmentation (Figure 2L) were observed. The direction of these changes was maintained in the two individuals who underwent a third polysomnography (Figure S1). There were no significant changes in the non-carrier group (Figure S2). When stratified for genotypes, we observed no major differences across ALS-causing mutations, although these analyses remained exploratory in non-*C9orf72* carriers due to limited sample size (Figures S3–S5). There were no major changes in medication that could underlie the observed effects (Table 3). Thus, the alteration in sleep stages observed in presymptomatic ALS gene carriers worsens over time.

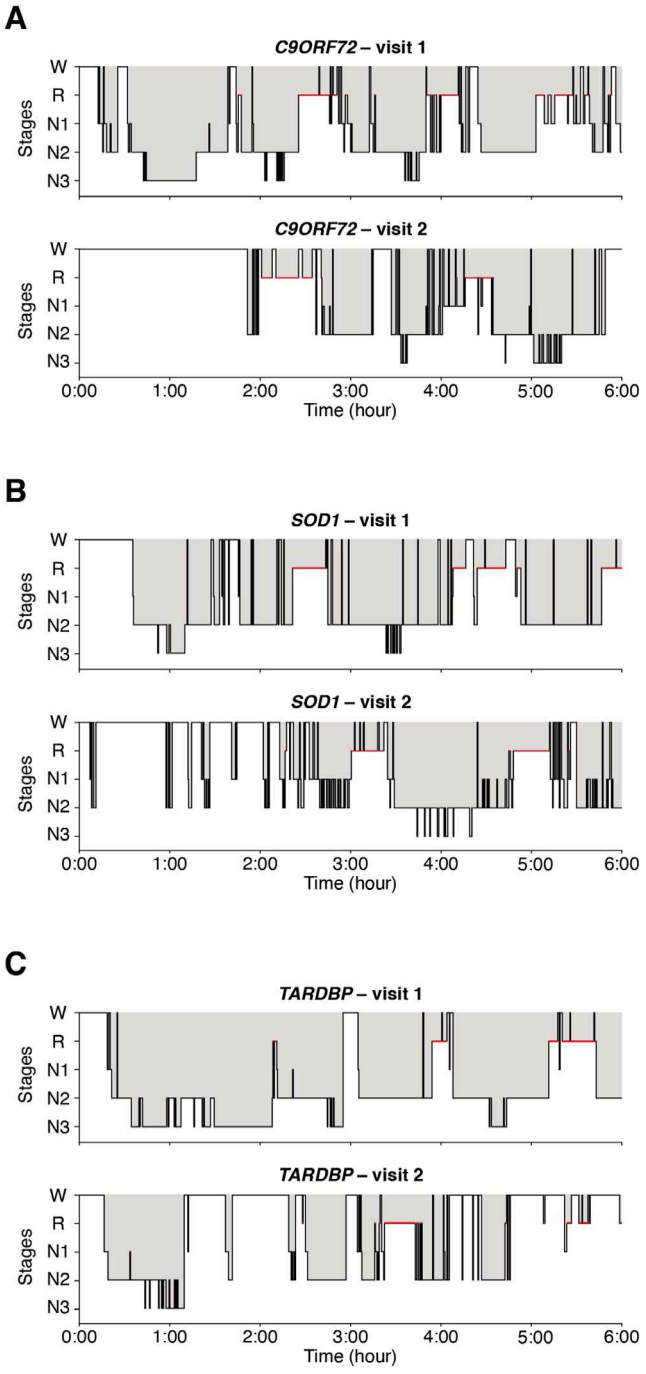


FIGURE 1 | Representative hypnograms of premanifest ALS gene carriers across both visits. (A) Hypnogram of a *C9orf72* premanifest gene carrier (case #09) at visit 1 (upper) and visit 2 (lower). (B) Hypnogram of a *SOD1* premanifest gene carrier (case #06) at visit 1 (upper) and visit 2 (lower). (C) Hypnogram of a *TARDBP* premanifest gene carrier (case #01) at visit 1 (upper) and visit 2 (lower).

3.2 | Premanifest Alterations in Sleep Microarchitecture

Altered sleep is also reflected in alterations in sleep-related electroencephalogram (EEG) hallmarks, including sleep spindles, slow oscillations, and K-complexes, that are critical for sleep functions. Using the polysomnography recordings, we observed a significant decrease in sleep spindle density (Figure 3A), slow wave oscillation density (Figure 3B), and K-complex density (Figure 3C). Here again, the direction of the changes in sleep microarchitecture was consistent in the two individuals who underwent a third visit (Figure 6) and in non-carriers (Figure 7). Similar to macro-architectural alterations, the observed directionality of change in microarchitecture was consistently observed when carriers were stratified across genotypes (Figures 8–10).

3.3 | Sleep Alterations and Their Independence From Motor Symptom Onset

One *C9orf72* gene carrier phenoconverted to clinically manifest ALS between the second and third visit (indicated by the red dot and solid red line in Figures 2 and 3 and Supporting Information). No specific divergence from the general sleep alteration was observed in this patient. To assess whether proximity to onset was related to worsening of sleep defects, we measured NF-L levels across visits. Three subjects showed pathologically high neurofilament levels (defined as a z-Score >1.0 at follow-up), suggestive of proximity to disease onset [3, 12]. The four subjects close to disease onset (three with pathological NF-L, one phenoconverter) did not show obvious distinct patterns in the worsening or extent of sleep alterations as compared to other subjects with normal NF-L levels (Figure 4A–C).

4 | Discussion

The primary aim of the present study was to assess longitudinal intra-individual changes in sleep architecture in gene carriers. In our previous study, we demonstrated that sleep patterns, including macrostructural and microstructural sleep architecture, differ between gene carriers and non-gene carriers. The present study extends these findings by focusing on longitudinal sleep changes within gene carriers over time. Here, we performed longitudinal follow-up polysomnography in presymptomatic ALS gene carriers and in family members with negative genetic testing. We observed a systematic progression of both macro- and

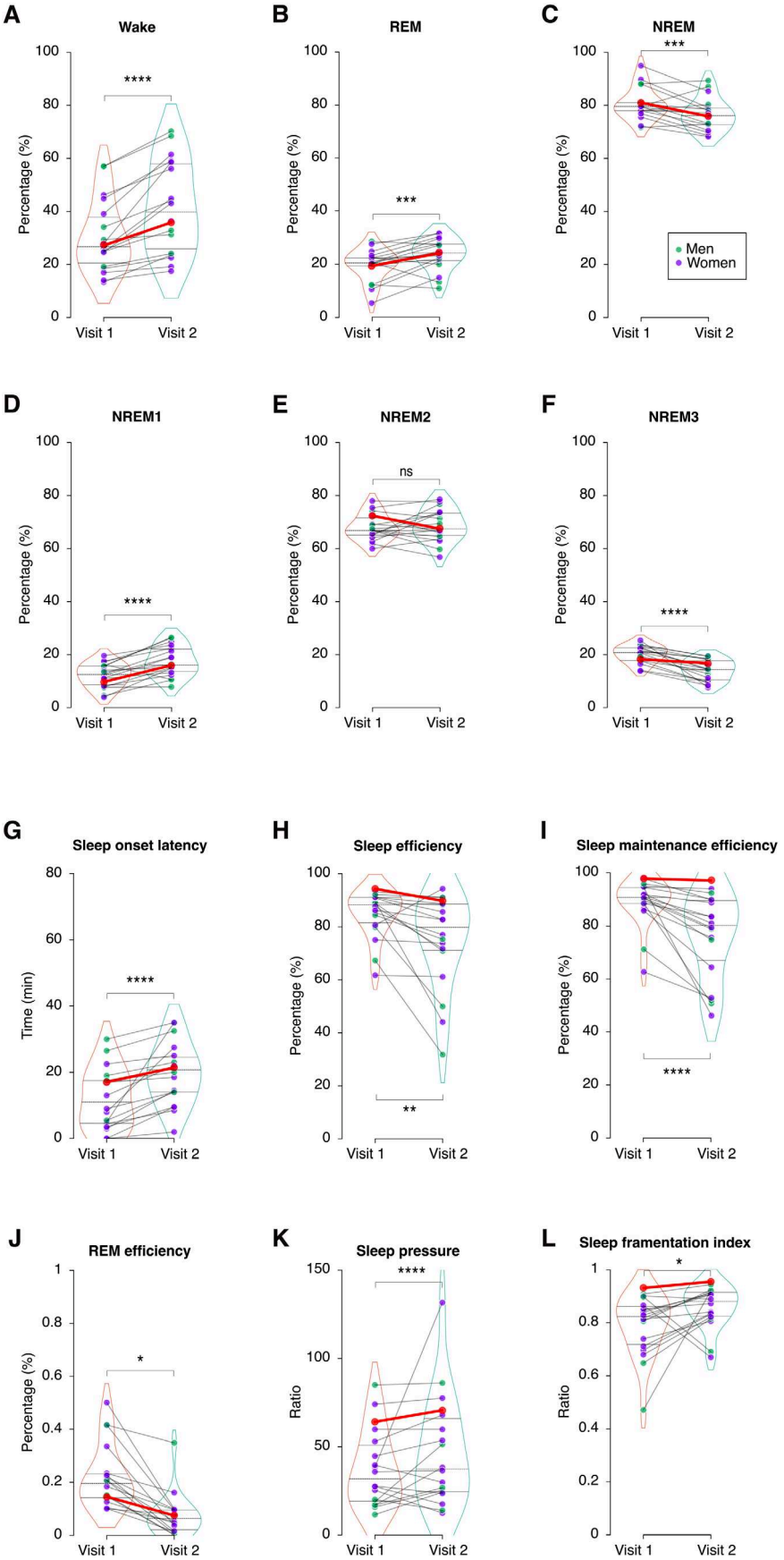


FIGURE 2 | Legend on next page.

FIGURE 2 | Quantification of sleep macroarchitecture across both visits. (A–L) Percentage of wake (A), REM (B), NREM (C), NREM1 (D), NREM2 (E) and NREM3 (F); sleep onset latency (latency to the first epoch of any sleep stage) (G); sleep efficiency (ratio of total sleep time to the time spent in bed) (H); sleep maintenance efficiency (ratio of sustained and continuous sleep after onset to total sleep time) (I); REM efficiency (ratio of REM sleep duration to total sleep time) (J); Sleep pressure (homeostatic drive to sleep that increases with wakefulness and dissipates during sleep) (K); and sleep fragmentation index (index of stage shifts or awakenings during sleep; higher values indicate disrupted sleep) (L) in premanifest ALS gene carriers between visit 1 and visit 2. In all panels, men are shown in green and women in purple. The woman who phenoconverted to clinically manifest ALS is indicated in red. * adj. $p_{value} < 0.05$, ** adj. $p_{value} < 0.01$, *** adj. $p_{value} < 0.001$, **** adj. $p_{value} < 0.0001$ were considered significant. Linear mixed model with multiple comparisons controlled using FDR-BKY correction. Men are shown in green and women in purple. Data are presented as median and interquartile ranges. Corrected p_{value} are shown.

TABLE 2 | Descriptive overview of polysomnographic outcomes at baseline and follow-up visits in the entire cohort of gene carriers across all mutations, excluding family controls.

PSG outcome	PSG visit 1 (mean ± SD)	PSG visit 2 (mean ± SD)	adj. p_{value}	adj. p_{value} *C9ORF72*
Wake	29.87 (±12.36)	40.75 (±16.82)	< 0.0001	< 0.0001
REM	19.37 (±5.46)	22.55 (±5.83)	0.0002	0.0011
NREM	80.61 (±5.51)	77.42 (±5.88)	0.0002	0.0011
NREM1	11.62 (±4.21)	16.57 (±5.59)	< 0.0001	0.0001
NREM2	67.84 (±4.55)	68.70 (±5.69)	0.1283	0.1669
NREM3	20.55 (±3.18)	14.73 (±3.91)	< 0.0001	< 0.0001
SOL	12.29 (±8.57)	19.29 (±9.02)	< 0.0001	0.0002
SE	84.77 (±8.25)	75.08 (±16.27)	0.0012	0.0239
SME	88.48 (±8.14)	77.04 (±14.95)	< 0.0001	< 0.0001
REM efficiency	0.21 (±0.12)	0.08 (±0.09)	0.0208	0.0677
Sleep pressure	35.90 (±19.94)	45.20 (±28.40)	< 0.0001	< 0.0001
SFI	0.79 (±0.11)	0.85 (±0.08)	0.0104	0.1615
dSSp	1.49 (±1.69)	0.67 (±0.66)	0.0017	0.0018
dSoS	3.33 (±3.65)	2.24 (±2.07)	0.0077	0.0055
dKc	5.72 (±3.61)	4.02 (±3.25)	< 0.0001	< 0.0001

Abbreviations: SOL: sleep onset latency; SE: sleep efficiency; SME: sleep maintenance efficiency; SFI: sleep fragmentation index; dSSp: sleep spindle density; dSoS: slow oscillation density; dKc: K-complex density; adj. p_{value}: adjusted p_{value}.

microarchitectural sleep alterations. However, this progression seemingly was independent of proximity to motor onset evaluated by presently used measures such as increased neurofilament levels or phenoconversion during the study. These results suggest that polysomnography could serve as an objective measurement of disease progression in clinically silent ALS.

The identification of frequent ALS-associated gene mutations has enabled the investigation of premanifest signs in individuals at high risk of developing ALS. To date, most studies in presymptomatic ALS gene carriers have been cross-sectional in nature (for review, see [13]). It is well established that presymptomatic gene carriers show imaging abnormalities; on this topic, longitudinal studies are available mostly for *C9orf72*. *C9orf72* gene carriers show atrophy in several subcortical regions—particularly the thalamus [14, 15]—as well as white-matter atrophy in the cervical spinal cord. Additional abnormalities include disrupted network activity [16] and white matter atrophy in the spinal cord [17]. Corticospinal abnormalities appear subtle but show slight progression over 18 months of follow-up [17]. Longitudinal studies demonstrated that subcortical atrophy, especially thalamic atrophy, is progressive and already significant by the third decade of life in both *C9orf72* gene carriers [18–20]. Our observation of progressive sleep deficits may therefore be related to this ongoing subcortical atrophy—particularly thalamic degeneration—in *C9orf72* gene carriers, as such changes are already present at the ages represented in our cohort. It is important to note that the sleep alterations observed in ALS are therefore probably independent of developmental alterations, which were recently considered critical in *C9orf72* ALS-FTD [21, 22], since they are seemingly progressive over the few years of our study.

The relatively small sample size represents a limitation of the present study. This is mainly attributable to the longitudinal design and the high effort associated with repeated polysomnographic assessments, which require participants to attend the

TABLE 3 | Descriptive table of the medication of individuals.

Case	Classification	Age at visit 1	Gender	Gene	Medication at baseline (daily dose)	Medication at Follow-up1 (daily dose)	Medication at Follow-up 2
01	Carrier	27	W	*TARDBP*	Amlodipine (5 mg), Levodopa/ Benserazide (100 mg)	Amlodipine (5 mg), Levodopa/ Benserazide (100 mg)	
02	Carrier	51	W	*C9ORF72*	Amlodipine (10 mg)	Amlodipine (10 mg), Candesartan (16 mg)	
03	Carrier	25	M	*C9ORF72*	—	—	
04	Carrier	22	M	*C9ORF72*	—	—	
05	Carrier	17	W	*FUS*	Enalapril (10 mg), Aripiprazole (10 mg), Daridorexant (50 mg)	Enalapril (10 mg), Aripiprazole (10 mg), Daridorexant (50 mg)	
06	Carrier	47	W	*SOD1*	Magnesium (400 mg), Levodopa/ Benserazidec(100 mg)	—	
07	Carrier	29	W	*FUS*	Opipramole (100 mg), Vitamin E	Opipramole (100 mg), Vitamin E	Riluzole (100 mg), Opipramole (100 mg)
08	Control	47	W	*C9ORF72*	L-Thyroxine (100 μg), Paroxetine (30 mg)	L-Thyroxine (75 μg), Paroxetine (30 mg)	
09	Carrier	33	W	*C9ORF72*	Simvastatin (60 mg)	Simvastatin (60 mg)	Simvastatin (60 mg)
10	Carrier	38	W	*C9ORF72*	Drospirenone/Estetrol (3/14,2 mg)	Drospirenone/Estetrol (3/14,2 mg)	
11	Carrier	47	M	*C9ORF72*	—	—	
12	Control	38	M	*GRN*	—	—	
14	Carrier	60	W	*C9ORF72*	Lamotrigine (150 mg)	Lamotrigine (150 mg)	
15	Control	48	W	*C9ORF72*	—	—	
16	Carrier	35	W	*SOD1*	—	—	
17	Carrier	32	W	*SOD1*	Vitamin E, Vitamin D, Magnesium (400 mg)	—	
18	Carrier	31	W	*C9ORF72*	—	—	
19	Carrier	44	W	*C9ORF72*	Erenumab (70 mg weekly) Sumatriptan (50 mg (as needed)), Naproxen (500 mg (as needed)), Melatonin (2 mg (as needed, not during PSG))	Erenumab (70 mg weekly) Rizatriptan (10 mg (as needed)), Naproxen (500 mg (as needed)), Melatonin (2 mg (as needed, not during PSG))	
20	Carrier	29	W	*C9ORF72*	—	—	

(Continues)

TABLE 3 | (Continued)

Case	Classification	Age at visit 1	Gender	Gene	Medication at baseline (daily dose)	Medication at Follow-up1 (daily dose)	Medication at Follow-up 2
21	Carrier	31	M	*C9ORF72*	—	—	
22	Carrier	41	W	*C9ORF72*	—	—	

Note: Medications are reported by active substance per visit. The respective dose is provided in brackets; unless otherwise stated, doses refer to the daily dose. For medications not taken daily, the dosing frequency is indicated separately in brackets. "–" indicates no current medication at the time of the visit. "–" indicates no current medication at the time of the visit.
Abbreviations: W: woman; M: man; mg: milligrammes; µg: micrograms.

hospital for overnight recordings. This is particularly challenging in presymptomatic gene carriers who are otherwise healthy, often working in regular jobs, and may have family and other everyday responsibilities. These factors make recruitment and retention difficult and limit the feasibility of substantially larger longitudinal polysomnography cohorts. This may have introduced selection bias, as individuals willing and able to undergo repeated in-hospital assessments may not fully represent the broader population of gene carriers.

Psychiatric symptoms, psychological distress, and medication may influence sleep architecture and therefore represent potential confounders in the present cohort. Although relevant medical history and medication use were documented during clinical assessment, psychiatric symptoms such as anxiety or mood disturbances were not systematically assessed using standardised questionnaires. Due to the small sample size and exploratory nature of the study, these variables were not included as covariates in the statistical models. This should be considered when interpreting the findings. In addition, we cannot completely rule out that the progression observed in gene carriers is related to ageing. Indeed, it is already well known that sleep micro- and macroarchitecture change with ageing, with a particular reduction in deep sleep and a reduction in the density of sleep spindles and slow waves [23, 24]. However, our analyses show a tendency towards an increased proportion of REM sleep in gene carriers over time, which is inconsistent with a purely age-related process, and is consistent with the increased proportion of REM sleep that we detected in ALS patients [7]. In addition, the physiological effects of ageing on sleep manifest over decades; a change of this extent in such a short period of time is unusual and is likely to be related to a disease or premature ageing. Indeed, we did not observe significant alterations in sleep patterns in the 3 non-carrier individuals included. However, future studies should include larger populations to disentangle the age effect from genetic background effects.

Sleep parameters are additionally influenced by inter-individual variability and methodological factors. Although established normative data from healthy populations provide useful context for parameters such as sleep onset latency, sleep maintenance, REM sleep measures, and sleep efficiency, direct comparison with such values is limited in the present cohort. This is due to the wide age range, variable intervals between assessments, small sample size, and the use of single-night polysomnography at each assessment. The latter is particularly relevant because the potential first-night effect may influence sleep continuity, sleep onset latency, and REM sleep parameters, thereby limiting direct comparability with normative values of physiological sleep.

Presymptomatic gene carriers also show discrete alterations in cognitive function, although neuropsychological performance is generally within the normal range before symptom onset in *C9orf72* carriers [20]. The reported phenotypes principally involve deficits in verbal fluency [25, 26]. In addition to cognitive signs, subtle oculomotor impairments [26] have also been demonstrated, as well as metabolic and sleep abnormalities [7, 27–29], but their evolution as individuals approach disease onset remains poorly characterised. Our study did not allow us to relate the progression of cognitive or metabolic dysfunction

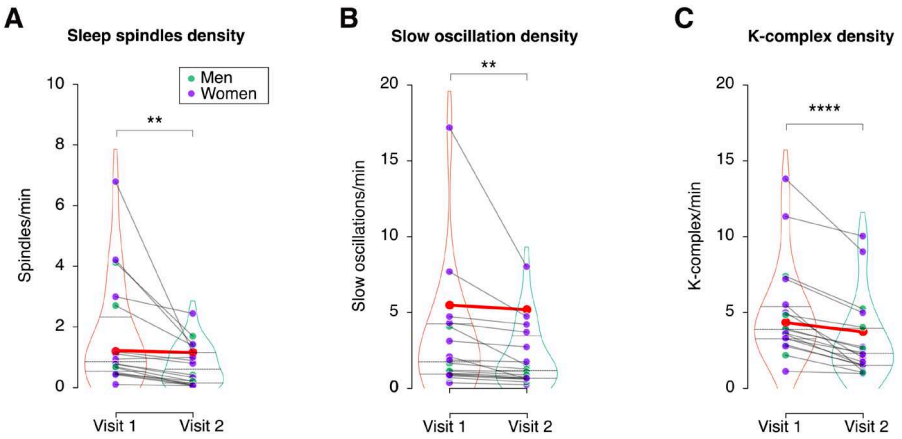


FIGURE 3 | Quantification of sleep microarchitecture across both visits. (A–C) Quantification of sleep spindle density (A), Slow oscillation density (B), and K-complex density (C) in premanifest ALS gene carriers between visit 1 and visit 2. In all panels, men are shown in green and women in purple. The woman who phenoconverted to clinically manifest ALS is indicated in red. * adj. $p_{value} < 0.05$, **** adj. $p_{value} < 0.0001$ were considered significant. Linear mixed model with multiple comparisons controlled using FDR-BKY correction. Men are shown in green and women in purple. Data are presented as median and interquartile ranges. Corrected p_{value} are shown.

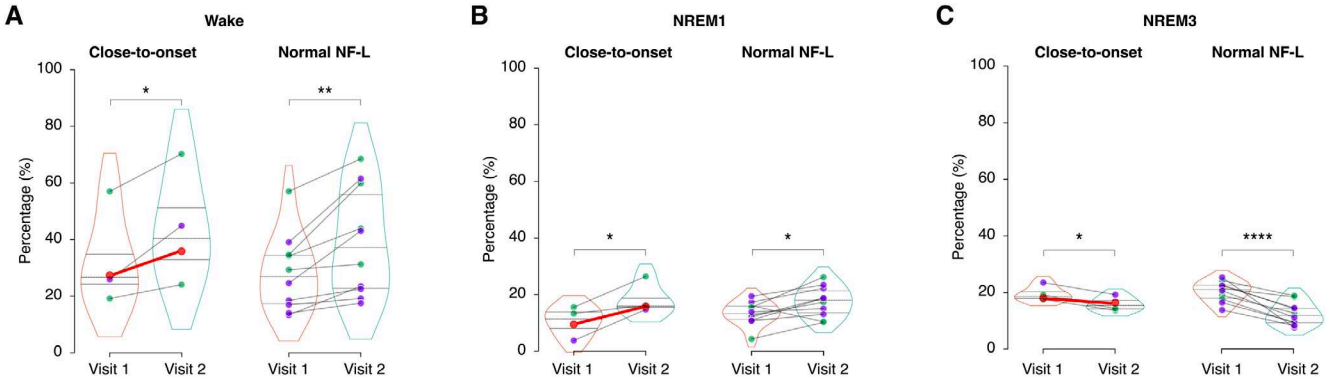


FIGURE 4 | Stratification across proximity to disease onset. (A–C) Percentage of wake (A), NREM1 (B), and NREM3 (C) in premanifest ALS gene carriers either close to disease onset (either phenoconversion during study or abnormally high neurofilament levels) and other patients (no phenoconversion and normal neurofilament levels). In all panels, men are shown in green and women in purple. The woman who phenoconverted to clinically manifest ALS is indicated in red. We observed similar worsening of sleep defects independent of proximity to disease onset. * adj. $p_{value} < 0.05$ were considered significant. For the normal NF-L group, a linear mixed model with multiple comparisons controlled using FDR-BKY correction. For the close-to-onset group, differences were analysed using the Wilcoxon-Mann–Whitney rank-sum test. Men are shown in green and women in purple. Data are presented as median and interquartile ranges. Corrected p_{value} are shown.

to sleep alterations, largely because these signs remain subtle at this stage and would require longer follow-up and larger sample sizes. This is consistent with the broader ALS literature, in which most available data remain cross-sectional [13]. The definition of mild motor impairment (MMI) is relatively recent [4, 30], and further longitudinal studies are needed to improve understanding of early disease trajectories.

In our study, we did not find an obvious relationship between the progression of sleep abnormalities and phenoconversion. In addition, the recently proposed Miami Framework highlights multiple dimensions of the premanifest ALS period—including frontotemporal and extrapyramidal domains [31], and it remains to be determined whether sleep-related changes are linked to these additional phenotypic dimensions.

Overall, our study provides the first evidence that EEG-related abnormalities progress during the premanifest phase of ALS. These changes might be the basis of neurochemical abnormalities, such as changes in the orexin or MCH system, which can be quantified and finally used as predictive tools [7]. These findings also emphasise the need for multimodal characterisation of at-risk individuals to clarify how sleep alterations and their neurochemical consequences relate to disease onset and progression.

Author Contributions

Christina Lang: conceptualization, investigation, funding acquisition, writing – original draft, methodology. **Simon J. Guillot:** investigation, methodology, visualization, data curation, writing – review and editing. **Antje Knehr:** investigation, methodology, project administration, writing – review and editing. **Patrick Weydt:** conceptualization, methodology, writing – review and editing, project administration. **Johannes Dorst:** conceptualization, methodology, writing – review and editing, project administration. **Hayrettin Tumani:** investigation. **Albert C. Ludolph:** conceptualization, investigation, funding acquisition, writing

– original draft, methodology, validation, supervision, resources, project administration. **Luc Dupuis:** conceptualization, funding acquisition, writing – original draft, methodology, validation, visualization, formal analysis, project administration, supervision. **Matei Bolborea:** conceptualization, funding acquisition, writing – original draft, methodology, validation, visualization, formal analysis, project administration, supervision.

Acknowledgements

The authors thank the volunteers and their families for their participation in these studies. Fondation Anne-Marie et Roger Dreyfus (hosted by Fondation de France) provided salary for S.J.G. C.L. was supported by a salary from the Charcot Stiftung. This work was funded by Agence Nationale de la Recherche (ANR-24-CE37-4064), by the Interdisciplinary Thematic Institute NeuroStra, as part of the ITI 2021-2028 (Idex Unistra ANR-10-IDEX-0002, ANR-20-SFRI-0012), Fondation Thierry Latran, Association Francaise de Recherche sur la sclérose latérale amyotrophique, the Association Française contre les Myopathies (AFM-Téléthon, #28944), TargetALS and JPND (HiCALS project). L.D. is a founding member of Institut Charcot, and received funding for this work.

Funding

This work was supported by Agence Nationale de la Recherche (ANR-24-CE37-4064, ANR-10-IDEX-0002, ANR-20-SFRI-0012, and JPND HiCALS); Association pour la Recherche sur la Sclérose Latérale Amyotrophique et autres Maladies du Motoneurone (DORALS, Institut Charcot); French Muscular Dystrophy Association (28944); and Target ALS.

Conflicts of Interest

The authors declare no conflicts of interest.

Data Availability Statement

All numerical data are provided in a spreadsheet in the Supporting Information (Lang_Guillot_data_file.csv).

References

1. S. A. Goutman, O. Hardiman, A. Al-Chalabi, et al., "Emerging Insights Into the Complex Genetics and Pathophysiology of Amyotrophic Lateral Sclerosis," *Lancet Neurology* 21 (2022): 465–479.

2. S. A. Goutman, O. Hardiman, A. Al-Chalabi, et al., "Recent Advances in the Diagnosis and Prognosis of Amyotrophic Lateral Sclerosis," *Lancet Neurology* 21 (2022): 480–493.

3. P. Weydt, P. Oeckl, A. Huss, et al., "Neurofilament Levels as Biomarkers in Asymptomatic and Symptomatic Familial Amyotrophic Lateral Sclerosis," *Annals of Neurology* 79 (2016): 152–158.

4. M. Benatar, V. Granit, P. M. Andersen, et al., "Mild Motor Impairment as Prodromal State in Amyotrophic Lateral Sclerosis: A New Diagnostic Entity," *Brain* 145 (2022): 3500–3508.

5. A. Ludolph, L. Dupuis, E. Kasarskis, F. Steyn, S. Ngo, and C. McDermott, "Nutritional and Metabolic Factors in Amyotrophic Lateral Sclerosis," *Nature Reviews. Neurology* 19 (2023): 511–524.

6. S. Abrahams, "Neuropsychological Impairment in Amyotrophic Lateral Sclerosis-Frontotemporal Spectrum Disorder," *Nature Reviews. Neurology* 19 (2023): 655–667.

7. S. J. Guillot, C. Lang, M. Simonot, et al., "Early-Onset Sleep Alterations Found in Patients With Amyotrophic Lateral Sclerosis Are Ameliorated by Orexin Antagonist in Mouse Models," *Science Translational Medicine* 17 (2025): eadm7580.

8. C. Lang, S. J. Guillot, D. Lule, et al., "Early Brain-Wide Disruption of Sleep Microarchitecture in Amyotrophic Lateral Sclerosis," *Journal of Clinical Investigation* 136 (2025): e194555.

9. R. B. Berry, R. Budhiraja, D. J. Gottlieb, et al., "Rules for Scoring Respiratory Events in Sleep: Update of the 2007 AASM Manual for the Scoring of Sleep and Associated Events. Deliberations of the Sleep Apnea Definitions Task Force of the American Academy of Sleep Medicine," *Journal of Clinical Sleep Medicine* 8 (2012): 597–619.

10. R. Vallat and M. P. Walker, "An Open-Source, High-Performance Tool for Automated Sleep Staging," *eLife* 10 (2021): e70092.

11. S. Halbgebauer, V. Klose, B. Fazeli, et al., "Neurofilament Light Chain Reference Values in Serum and Cerebrospinal Fluid: A Bi-Compartmental Analysis in Neurological Diseases," *Journal of Neurology* 272 (2025): 535.

12. M. Benatar, J. Wuu, P. M. Andersen, V. Lombardi, and A. Malaspina, "Neurofilament Light: A Candidate Biomarker of Presymptomatic Amyotrophic Lateral Sclerosis and Phenoconversion," *Annals of Neurology* 84 (2018): 130–139.

13. M. Benatar, M. R. Turner, and J. Wuu, "Presymptomatic Amyotrophic Lateral Sclerosis: From Characterization to Prevention," *Current Opinion in Neurology* 36 (2023): 360–364.

14. P. Bede, D. Lule, H. P. Muller, et al., "Presymptomatic Grey Matter Alterations in ALS Kindreds: A Computational Neuroimaging Study of Asymptomatic C9orf72 and SOD1 Mutation Carriers," *Journal of Neurology* 270 (2023): 4235–4247.

15. J. D. Rohrer, J. M. Nicholas, D. M. Cash, et al., "Presymptomatic Cognitive and Neuroanatomical Changes in Genetic Frontotemporal Dementia in the Genetic Frontotemporal Dementia Initiative (GENFI) Study: A Cross-Sectional Analysis," *Lancet Neurology* 14 (2015): 253–262.

16. M. Trubshaw, C. Gohil, E. Edmond, et al., "Divergent Brain Network Activity in Asymptomatic C9orf72 and SOD1 Variant Carriers Compared With Established Amyotrophic Lateral Sclerosis," *Human Brain Mapping* 46 (2025): e70345.

17. G. Querin, P. Bede, M. M. El Mendili, et al., "Presymptomatic Spinal Cord Pathology in c9orf72 Mutation Carriers: A Longitudinal Neuroimaging Study," *Annals of Neurology* 86 (2019): 158–167.

18. V. Planche, B. Mansencal, V. Fonov, et al., "Anatomical Progression of Genetic Frontotemporal Lobar Degeneration Across the Lifespan," *Brain* 148 (2025): 3880–3892.

19. K. van Veenhuijzen, H. H. G. Tan, A. D. Nitert, et al., "Longitudinal Magnetic Resonance Imaging in Asymptomatic C9orf72 Mutation Carriers Distinguishes Phenoconverters to Amyotrophic Lateral Sclerosis or Amyotrophic Lateral Sclerosis With Frontotemporal Dementia," *Annals of Neurology* 97 (2025): 281–295.

20. A. M. Staffaroni, M. Quintana, B. Wendelberger, et al., "Temporal Order of Clinical and Biomarker Changes in Familial Frontotemporal Dementia," *Nature Medicine* 28 (2022): 2194–2206.

21. E. Hendricks, A. M. Quihuis, S. T. Hung, et al., "The C9ORF72 Repeat Expansion Alters Neurodevelopment," *Cell Reports* 42 (2023): 112983.

22. E. Finger, R. Malik, M. Bocchetta, et al., "Neurodevelopmental Effects of Genetic Frontotemporal Dementia in Young Adult Mutation Carriers," *Brain* 146 (2023): 2120–2131.

23. R. F. Helfrich, B. A. Mander, W. J. Jagust, R. T. Knight, and M. P. Walker, "Old Brains Come Uncoupled in Sleep: Slow Wave-Spindle Synchrony, Brain Atrophy, and Forgetting," *Neuron* 97 (2018): 221–230.

24. K. R. Peters, L. B. Ray, S. Fogel, V. Smith, and C. T. Smith, "Age Differences in the Variability and Distribution of Sleep Spindle and Rapid Eye Movement Densities," *PLoS One* 9 (2014): e91047.

25. D. E. Lule, H. P. Muller, J. Finsel, et al., "Deficits in Verbal Fluency in Presymptomatic C9orf72 Mutation Gene Carriers-a Developmental Disorder," *Journal of Neurology, Neurosurgery, and Psychiatry* 91 (2020): 1195–1200.

26. A. Behler, A. Knehr, J. Finsel, et al., "Eye Movement Alterations in Presymptomatic C9orf72 Expansion Gene Carriers," *Journal of Neurology* 268 (2021): 3390–3399.

27. K. Xia, S. Witzel, C. Witzel, et al., "Mutation-Specific Metabolic Profiles in Presymptomatic Amyotrophic Lateral Sclerosis," *European Journal of Neurology* 30 (2022): 87–95.

28. I. Lee, M. A. Garret, J. Wuu, et al., "Body Mass Index Is Lower in Asymptomatic C9orf72 Expansion Carriers but Not in SOD1 Pathogenic Variant Carriers Compared to Gene Negatives," *Amyotroph Lateral Scler Frontotemporal Degener* 25 (2024): 672–679.

29. H. J. Westeneng, K. van Veenhuijzen, R. A. van der Spek, et al., "Associations Between Lifestyle and Amyotrophic Lateral Sclerosis Stratified by C9orf72 Genotype: A Longitudinal, Population-Based, Case-Control Study," *Lancet Neurology* 20 (2021): 373–384.

30. M. Benatar, X. Cai, M. P. McDermott, et al., "Proposed Research Criteria for Mild Motor Impairment as a Prodromal Syndrome in Amyotrophic Lateral Sclerosis," *Neurology* 105 (2025): e213917.

31. M. Benatar, J. Wuu, E. D. Huey, et al., "The Miami Framework for ALS and Related Neurodegenerative Disorders: An Integrated View of Phenotype and Biology," *Nature Reviews. Neurology* 20 (2024): 364–376.

Supporting Information

Additional supporting information can be found online in the Supporting Information section. **Data S1:** ene70755-sup-0001-Supinfo-1.docx. **Data S2:** ene70755-sup-0002-Supinfo-2.csv. **Figure S1:** Quantification of sleep macroarchitecture across three visits. (A–L) Percentage of wake (A), REM (B), NREM (C), NREM1 (D), NREM2 (E), and NREM3 (F); sleep onset latency (latency to the first epoch of any sleep stage) (G); Sleep efficiency (ratio of total sleep time to the time spent in bed) (H); sleep maintenance efficiency (ratio of sustained and continuous sleep after onset to total sleep time) (I); REM efficiency (ratio of REM sleep duration to total sleep time) (J); Sleep pressure (homeostatic drive to sleep that increases with wakefulness and dissipates during sleep) (K); and sleep fragmentation index (index of stage shifts or awakenings during sleep; higher values indicate disrupted sleep) (L) in the two volunteers who underwent three visits (2 women). The woman who phenoconverted to clinically manifest ALS is indicated in red. This figure is presented descriptively; statistical analysis was not performed given the small sample size ($n = 2$). Figure 2 Quantification of sleep macroarchitecture across both visits in non-carriers. (A–L) Percentage of wake (A), REM (B), NREM (C), NREM1 (D), NREM2 (E), and NREM3 (F); sleep onset latency (latency to the first epoch of any sleep stage) (G); sleep efficiency (ratio of total sleep time to the time spent in bed) (H); sleep maintenance efficiency (ratio of sustained and continuous sleep after onset to total sleep time) (I); REM efficiency (ratio of REM sleep duration to total sleep time) (J); Sleep pressure (homeostatic drive to sleep that increases with wakefulness and dissipates during sleep) (K); and sleep fragmentation index (indice of stage shifts or awakenings during sleep; higher values indicate disrupted sleep) (L) in premanifest ALS gene carriers between visit 1 and visit 2. In all panels, men are shown in green and women in purple. No significant difference is observed (Wilcoxon-Mann–Whitney rank-sum test). Figure 3 Quantification of sleep macroarchitecture across both visits in *C9orf72* carriers. (A–L) Percentage of wake (A), REM (B), NREM (C), NREM1 (D), NREM2 (E), and NREM3 (F); sleep onset latency (latency to the first epoch of any sleep stage) (G); sleep efficiency (ratio of total sleep time to the time spent in bed) (H); sleep maintenance efficiency (ratio of sustained and continuous sleep after onset to total sleep time) (I); REM efficiency (ratio of REM sleep duration to total sleep time) (J); Sleep pressure (homeostatic drive to sleep that increases with wakefulness and dissipates during sleep) (K); and sleep fragmentation index (indice of stage shifts or awakenings during sleep; higher values indicate disrupted sleep) (L) in premanifest ALS gene carriers between visit 1 and visit 2. In all panels, men are shown in green and women in purple. The woman who phenoconverted to clinically manifest ALS is indicated in red. ** adj. $p_{value} < 0.01$, *** adj. $p_{value} < 0.001$, **** adj. $p_{value} < 0.0001$ were considered significant. Linear mixed model with multiple comparisons controlled using FDR-BKY correction. Men are shown in green and women in purple. Data are presented as median and interquartile ranges. Corrected p_{value} are shown. Figure 4 Quantification of sleep macroarchitecture across both visits in *SOD1* carriers. (A–L) Percentage of wake (A), REM (B), NREM (C), NREM1 (D), NREM2 (E), and NREM3 (F); sleep onset latency (latency to the first epoch of any sleep stage) (G); sleep efficiency (ratio of total sleep time to the time spent in bed) (H); sleep maintenance efficiency (ratio of sustained and continuous sleep after onset to total sleep time) (I); REM efficiency (ratio of REM sleep duration to total sleep time) (J); Sleep pressure (homeostatic drive to sleep that increases with wakefulness and dissipates during sleep) (K); and sleep fragmentation index (indice of stage shifts or awakenings during sleep; higher values indicate disrupted sleep) (L) in premanifest ALS gene carriers between visit 1 and visit 2. In all panels, men are shown in green and women in purple. Figure 5 Quantification of sleep macroarchitecture across both visits in non-*C9orf72/SOD1* gene carriers. (A–L) Percentage of wake (A), REM (B), NREM (C), NREM1 (D), NREM2 (E), and NREM3 (F); sleep onset latency (latency to the first epoch of any sleep stage) (G); sleep efficiency (ratio of total sleep time to the time spent in bed) (H); sleep maintenance efficiency (ratio of sustained and continuous sleep after onset to total sleep time) (I); REM efficiency (ratio of REM sleep duration to total sleep time) (J); Sleep pressure (homeostatic drive to sleep that increases with wakefulness and dissipates during sleep) (K); and sleep fragmentation index (indice of stage shifts or awakenings during sleep; higher values indicate disrupted sleep) (L) in premanifest ALS gene carriers between visit 1 and visit 2. In all panels, men are shown in green and women in purple. Figure 6 Quantification of sleep microarchitecture across three visits. (A–C) Quantification of sleep spindle density (A), Slow oscillation density (B), and K-complex density (C) in the two volunteers who underwent three visits (2 women). The woman who phenoconverted to clinically manifest ALS is indicated in red. This figure is presented descriptively; statistical analysis was not performed given the small sample size ($n = 2$). Figure 7 Quantification of sleep microarchitecture across both visits in non-carriers. (A–C) Quantification of sleep spindle density (A), Slow oscillation density (B), and K-complex density (C) in premanifest ALS gene carriers between visit 1 and visit 2. In all panels, men are shown in green and women in purple. No significant difference is observed (Wilcoxon-Mann–Whitney rank-sum test). Figure 8 Quantification of sleep microarchitecture across both visits in *C9orf72* carriers. (A–C) Quantification of sleep spindle density (A), Slow oscillation density (B), and K-complex density (C) in premanifest ALS gene carriers between visit 1 and visit 2. In all panels, men are shown in green and women in purple. ** adj. $p_{value} < 0.01$, **** adj. $p_{value} < 0.0001$ were considered significant. A linear mixed model with multiple comparisons controlled using FDR-BKY correction was performed. Men are shown in green and women in purple. Data are presented as median and interquartile ranges. Corrected p_{value} are shown. Figure 9 Quantification of sleep microarchitecture across both visits in *SOD1* carriers. (A–C) Quantification of sleep spindle density (A), Slow oscillation density (B), and K-complex density (C) in premanifest ALS gene carriers between visit 1 and visit 2. In all panels, men are shown in green and women in purple. Figure 10 Quantification of sleep microarchitecture across both visits in non-*C9orf72/SOD1* gene carriers. (A–C) Quantification of sleep spindle density (A), Slow oscillation density (B), and K-complex density (C) in premanifest ALS gene carriers between visit 1 and visit 2. In all panels, men are shown in green and women in purple.